Topological Isomerism in Three-Dimensional Covalent Organic Frameworks

Yaozu Liu, Jingwei Li, Jia Lv, Zitao Wang, Jinquan Suo, Junxia Ren, Jianchuan Liu, Dong Liu, Yujie Wang, Valentin Valtchev, et al.

▶ **To cite this version:**

Yaozu Liu, Jingwei Li, Jia Lv, Zitao Wang, Jinquan Suo, et al.. Topological Isomerism in Three-Dimensional Covalent Organic Frameworks. Journal of the American Chemical Society, 2023, 145 (17), pp.9679-9685. 10.1021/jacs.3c01070 . hal-04280289

HAL Id: hal-04280289
https://hal.science/hal-04280289

Submitted on 10 Nov 2023

HAL is a multi-disciplinary open access archive for the deposit and dissemination of scientific research documents, whether they are published or not. The documents may come from teaching and research institutions in France or abroad, or from public or private research centers.

L'archive ouverte pluridisciplinaire **HAL**, est destinée au dépôt et à la diffusion de documents scientifiques de niveau recherche, publiés ou non, émanant des établissements d'enseignement et de recherche français ou étrangers, des laboratoires publics ou privés.

Topological Isomerism in Three-Dimensional Covalent Organic Frameworks

Yaozu Liu,[†,§] Jingwei Li,[‡,§] Jia Lv,[‡] Zitao Wang,[†] Jinquan Suo,[†] Junxia Ren,[†] Jianchuan Liu,[†] Dong Liu,[‡] Yujie Wang,*[,†] Valentin Valtchev,[∥] Shilun Qiu,[†] Daliang Zhang,*[,‡] and Qianrong Fang*[,†]

[†]State Key Laboratory of Inorganic Synthesis and Preparative Chemistry, Jilin University, Changchun 130012, P. R. China

[‡] Multi-scale Porous Materials Center, Institute of Advanced Interdisciplinary Studies & School of Chemistry and Chemical Engineering, Chongqing University, Chongqing 400044, P. R. China

[∥]Qingdao Institute of Bioenergy and Bioprocess Technology, Chinese Academy of Sciences Qingdao, Shandong 266101, P. R. China; Normandie Univ, ENSICAEN, UNICAEN, CNRS, Laboratoire Catalyse et Spectrochimie, Caen 14050, France

Supporting Information Placeholder

ABSTRACT: Although isomerism is a typical and significant phenomenon in organic chemistry, it is rarely found in covalent organic framework (COF) materials. Herein, for the first time, we report a controllable synthesis of topological isomers in three-dimensional COFs via a distinctive tetrahedral building unit under different solvents. Based on this strategy, both isomers with **dia** or **qtz** net (termed JUC-620 and JUC-621) have been obtained, and their structures are determined by combining powder X-ray diffraction and transmission electron microscopy. Remarkably, these architectures show a distinct difference in their porous features, e.g., JUC-621 with **qtz** net exhibits permanent mesopores (up to ~ 23 Å) and high surface area (~ 2060 $m^2 g^{-1}$), which far surpasses those of JUC-620 with **dia** net (pore size of ~12 Å and surface area of 980 $m^2 g^{-1}$). Furthermore, mesoporous JUC-621 can remove dye molecules efficiently and achieves excellent iodine adsorption (up to 6.7 g g^{-1}), which is 2.3 times that of microporous JUC-620 (~2.9 g g^{-1}). This work thus provides a new way for constructing COF isomers and promotes structural diversity and promising applications of COF materials.

INTRODUCTION

Isomerism has been found to be existed widely in organic chemistry, in which there is the same chemical composition and molecular formula but the various spatial atomic arrangement.[1-2] These isomers, typically including small molecules and polymers, show unique physical and chemical properties, such as different thermal properties, boiling points, and crystallinity. Recently, Zhou et al. have defined the isomerism in metal-organic frameworks (MOFs), a typical crystalline porous material (CPM), as "framework isomers", and this interesting phenomenon has also attracted widespread attention.[3] Although isomerism in MOFs has already been found and their various chemical and physical properties have been studied accordingly, the type and number of isomers are still very limited, especially to other kinds of CPMs.

Covalent organic frameworks (COFs), an emerging class of CPMs, are composed of light elements (typically H, B, C, N, and O) linked by covalent bonds.[4-7] They feature well-defined pores and high specific surface areas that attracted extensive attention in different fields, such as heterogeneous catalysis,[8-9] adsorption and separation,[10-11] organic electronics,[12-13] and many others.[14-21] The development of three-dimensional (3D) COFs has lately become urgent research owing to their extensive advantages in interconnected pores and higher specific surface areas than two-dimensional (2D) counterparts.[22] For example, Wang, Sun, and co-workers provided a unique example of the phenomena of interpenetration isomers based on a well-known 3D COF, COF-300.[23] We have developed a series of 3D COFs with different topologies by using triangular prism triptycene linkers as node centers, such as JUC-564 with **stp** net,[24] JUC-568 and JUC-569 with **ceq** or **acs** net,[25] as well as JUC-596 and JUC-597 with **hea** net,[26] and constructed the first 3D COF with the zeolitic net (ZOF-1) by combining two kinds of tetrahedral building blocks with fixed or relatively free bond angles.[27] Although many efforts have been made, topological isomerism in 3D COFs has never been observed, which remains a great challenge.

Scheme 1. Energy scan analysis of tetrahedral building units as a function of dihedral angle.[a]

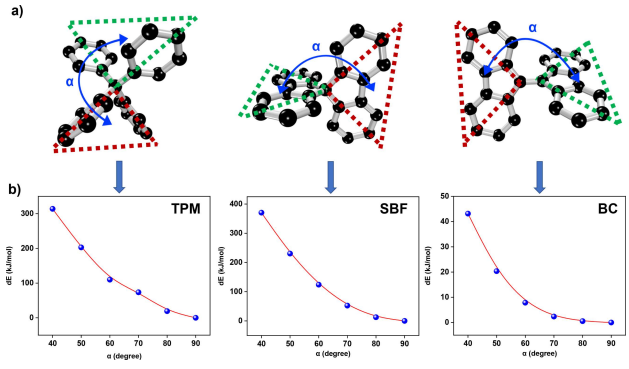

[a](a) Structures of tetraphenylmethane (TPM, left), 9,9′-spirobifluorene (SBF, middle), and 9,9′-bicarbazole (BC, right). (b) Potential energy scans of different tetrahedral building units based on the variable dihedral angle (α).

Scheme 2. Controllable synthesis of COF isomers by the condensation of BCTB-4CHO (a) and TFAPPM (b), JUC-620 with **dia** net (c) and JUC-621 with **qtz** net (d), and their transformation.

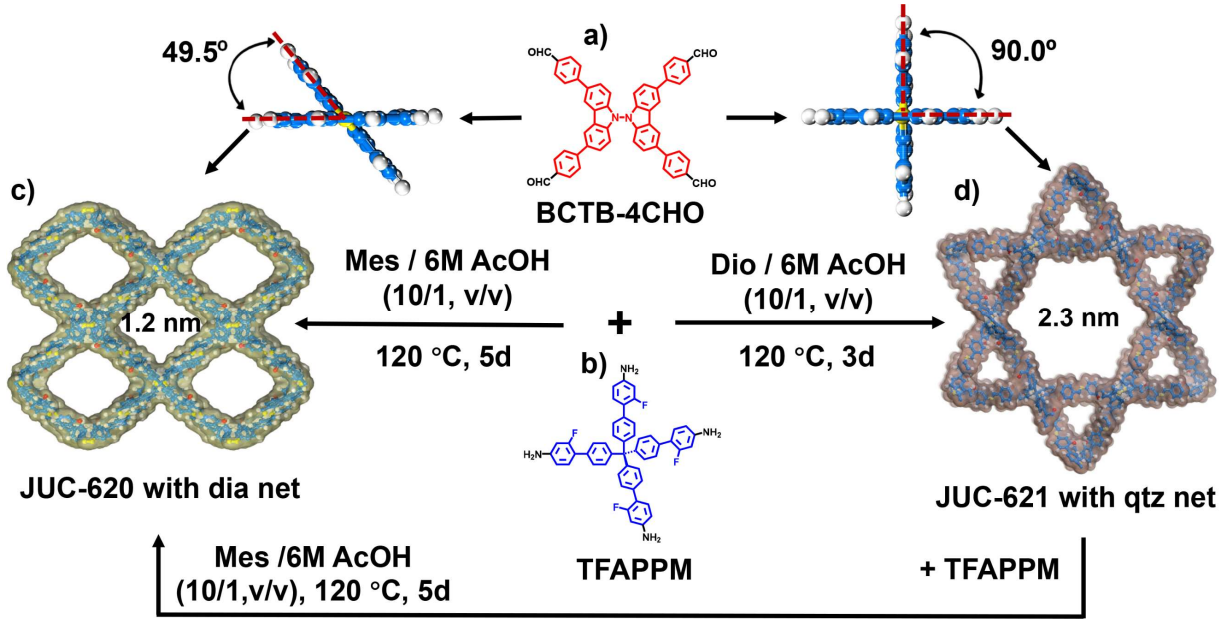

Herein, we report the first case of topological isomers in 3D COFs. By using a unique tetrahedral building unit, two 3D isomerous COFs with diamondoid (**dia**) or quartz (**qtz**) net, termed JUC-620 and JUC-621, have been successfully synthesized under different solvents, and their structures are determined by combining powder X-ray diffraction (PXRD) and transmission electron microscopy (TEM). Notably, JUC-621 represents the first COF with **qtz** net and shows stable mesopores with a pore size of 23 Å and a high BET surface area of 2060 $m^2\ g^{-1}$, which is much larger than those of its isomer, JUC-620 with **dia** net (pore size of 12 Å and BET surface area of 980 $m^2\ g^{-1}$). In addition, JUC-621 can remove dye molecules in water efficiently, and has a faster absorption rate (0.56 $g\ h^{-1}$) and a better adsorption capacity (6.7 $g\ g^{-1}$) for iodine (I_2), which far exceeds those of JUC-620 (absorption rate of 0.23 $g\ h^{-1}$ and uptake of 2.9 $g\ g^{-1}$).

RESULTS AND DISSCUSSION

In order to explore topological isomerism in 3D COFs, our strategy is based on the regulation of dihedral angles of tetrahedral building blocks by reticular chemistry.[28,29] By using Gaussian 09 software package, we calculated potential energy scans of three different tetrahedral building blocks. As shown in Scheme 1, tetraphenylmethane (TPM) as a typical tetrahedral building unit for **dia** net shows an energy increase (314 kJ mol^{-1}) as the dihedral angle changed (from 90° to 40°). Different from TPM, 9,9′-spirobifluorene (SBF) as a partially immobilized building unit exhibits an even more significant energy boost (370 kJ mol^{-1}) as the dihedral angle transform, resulting in the first 3D COF with the zeolitic net, ZOF-1.[27] Obviously, 9,9′-bicarbazole (BC) is also a partially immobilized building unit; however, it has much lower energy enlargement (43 kJ mol^{-1}) with the dihedral angle changed. Therefore, as a distinctive tetrahedral building unit, BC will probably tend to set up various architectures based on the partially flexible dihedral angle. According to this strategy, we designed and synthesized a derivative of BC containing aldehyde groups, 4,4′,4′′,4′′′-([9,9′-bicarbazole]-3,3′,6,6′-tetrayl)tetrabenzaldehyde (BCTB-4CHO, Scheme 2), and successfully produced two novel 3D COFs with topological isomerism by the condensation of BCTB-4CHO and tetra[(2-fluoro-4-aminophenyl)-phenyl]methane (TFAPPM).

Typically, isomers could be obtained under different synthetic conditions, such as solvents with different polarities.[30] Therefore, the synthesis of JUC-620 was carried out by suspending TFAPPM and BCTB-4CHO in a solution of 1,3,5-mesitylene (low polarity) with 12 M acetic acid aqueous solution, followed by heating at 120 °C for 5 days. Similarly, JUC-621 was synthesized in a solution of 1,4-dioxane (high polarity) with the same catalyst and temperature for 3 days (Scheme 2). Crystal morphologies were observed by combining scanning electron microscopy (SEM, Figures S1 and S2) and transmission electron microscopy (TEM, Figure 1). Both crystals exhibited a rhombus shape (~20 μm) and a hexagonal prism-

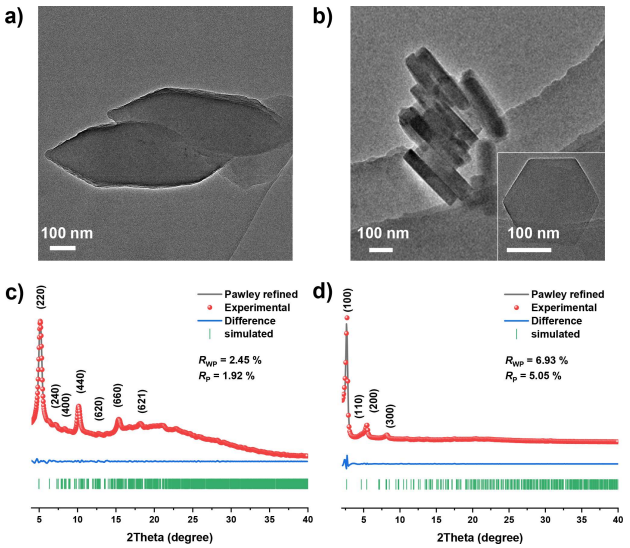

Figure 1. TEM and PXRD studies of JUC-620 and JUC-621. TEM images for JUC-620 (a) and JUC-621 (b). The scale bars represent 100 nm. Experimental and refined PXRD patterns of JUC-620 (c) and JUC-621 (d).

like shape (~2 μm), respectively. Fourier transform infrared (FT-IR) spectra exhibited new peaks around 1625 cm^{-1}, corresponding to typical C=N stretching vibrations, and the disappearance of N-H stretching band at 3310~3400 cm^{-1} and C=O stretching band at 1700 cm^{-1}, manifesting the complete conversion of Schiff-base polymerization (Figures S3 and S4). Furthermore, the solid-state ^{13}C cross-polarization magic-angle-spinning (CP/MAS) NMR spectra confirmed the presence of carbon from the C=N bond at 159 ppm for JUC-620 and 160 ppm for JUC-621, respectively (Figure S5). According to the thermogravimetric analysis (TGA), these COFs were thermally stable up to 400 °C under nitrogen (Figures S6-9). These products were stable in various organic solvents and aqueous solutions of strong acid (HCl with pH = 1) and strong base (NaOH with pH = 14, Figures S10 and S11) for at least 24 h.

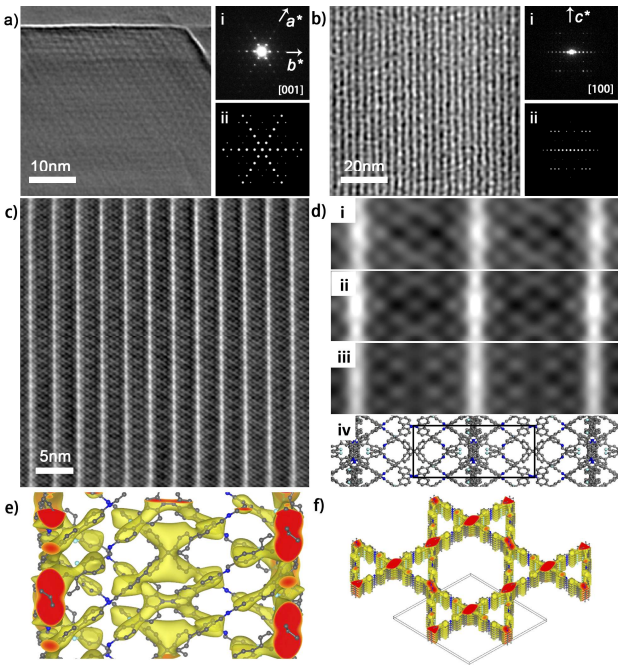

Figure 2. Structural analysis of JUC-621 by using TEM. (a) and (b), TEM images taken along [100] and [001] directions showing the strict and hexanol arranged channels, as well as the corresponding SAED patterns (i) and kinematical simulation results (ii) in both zone axes; (c) a high resolution iDPC-STEM image of JUC-621 acquired along the [100] zone axis; (d) lattice averaged image in *p*1 symmetry (i), *p*2*mm* symmetry imposed image (ii), simulated iDPC-STEM image (iii) and the corresponding structure projection (iv); (e) and (f), reconstructed 3D electrostatic potential map viewed along [110] and [001] zone axes, with the structure model superimposed. The boxes in (d) and (f) indicate one unit cell.

The precise structural determination and characteristics of both isomers were determined by combining PXRD patterns and TEM technique. To understand their crystal structures, rotation electron diffraction (RED) was first conducted for primary unit cells (Figure S12). The primary unit cells were further refined by PXRD data with the full profile pattern matching (Pawley) method (Figures 1c,d and S13). An orthorhombic unit cell with a = 43.287 Å, b = 58.125 Å, and c = 6.720 Å was obtained for JUC-620, where peaks at 5.09°, 7.34°, 8.46°, 10.18°, 12.63°, 15.30°, and 18.28° could be attributed to the (220), (240), (400), (440), (620), (660), and (621) Bragg peaks (Rp = 4.91% and ωRp = 3.74%). Similarly, the cell parameters of JUC-621 were determined as $a = b$ = 35.980 Å, c = 12.875 Å, $\alpha = \beta$ = 90.00°, and γ = 120.00°, where peaks at 2.74°, 4.74°, 5.47° and 8.23° of PXRD could be attributed to the (100), (110), (200), and (300) Bragg peaks (Rp = 6.93% and ωRp = 5.05%). The crystal system of JUC-621 was confirmed by selected area electron diffraction (SAED) patterns in [001] zone axis which exhibited 6*mm* symmetry (Figure 2a). Therefore, the crystal of JUC-621 was determined as hexagonal system. As shown in Figure S14, we were able to index 13 peaks from the PXRD pattern of JUC-621 after 6.00°, implying high crystallinity of the material.

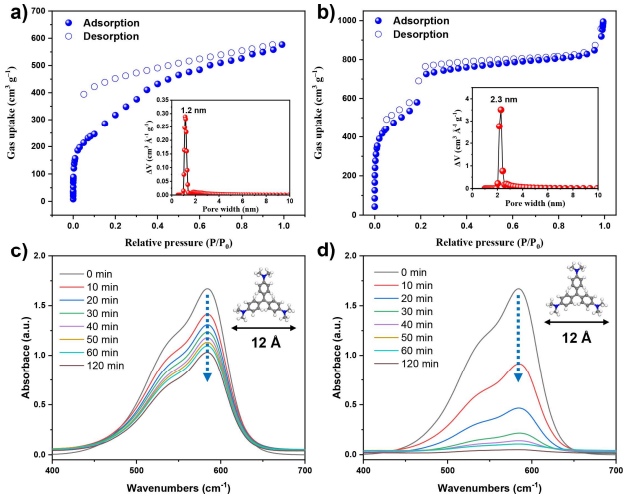

Figure 3. N_2 adsorption-desorption and UV/Vis spectrascopy. (a) N_2 adsorption-desorption isotherm of JUC-620 at 77 K, Inset: pore-size distribution of JUC-620. (b) N_2 adsorption-desorption isotherm of JUC-621 at 77 K, Inset: pore-size distribution of JUC-621. (c) UV/Vis spectra of fast adsorption of CV for JUC-620 in 120 min. (d) UV/Vis spectra of fast adsorption of CV for JUC-621 in 120 min.

The **dia** net is the most classic among all the 4-connected networks. A series of structure models were built according to the **dia** net and its interpenetration isomerism **dia**-cN, where N is the degree of interpenetration, N = 2 ~ 10 (Figure S15). Noticeable, JUC-620 is overlap (AA-stacking) but not staggered (AB-stacking) arrange on the *c*-axis (Figures S16 and S17), which is proved by only 6.38 Å length in *c*-axis of unit cells of RED. After geometrical energy minimizations by using the Materials Studio software package, the simulated PXRD pattern of the structure following 7-fold **dia** net (Figures S18-20) was in good agreement with the experimental results.

In order to determine the structure of JUC-621, high resolution TEM images were firstly conducted (Figure 2a,b). Hexagonal arranged white spots and periodically arranged white lines were observed in [001] and [100] directions of JUC-621, respectively. High-resolution iDPC-STEM images were taken to further gain insights into the crystal structure of JUC-621 (Figure 2c). The projection symmetry of JUC-621 along the [100] direction was determined as *p*2*mm* (φ_{res} = 11.4) by CRISP software (Figure S21).[31] On the other hand, the reflection condition 00*l*: *l* = 3*n* was also obtained from the Fast Furious Transform (FFT) of Figure 2c. Thus, the space group symmetry was determined as $P6_222$ (No. 180) or $P6_422$ (No. 181), a pair of enantiomorphic space groups. Using the square root of reflection intensities in SAED as amplitudes and the phase information obtained from iDPC-STEM, we could list 23 reflections as experimental structure factor (Table S1). The 3D electrostatic potential map (Figure 2e) could then be reconstructed through Vesta software,[32] in which BCTB-4CHO and TFAPPM were clearly identified (Figure S22). A 5-fold **qtz** net was built by connecting neighbor BCTB-4CHO and TFAPPM molecules. After geometry optimization, a model of JUC-621 in $P6_422$ space group as **qtz** net has been determined. The optimized unit cell parameters

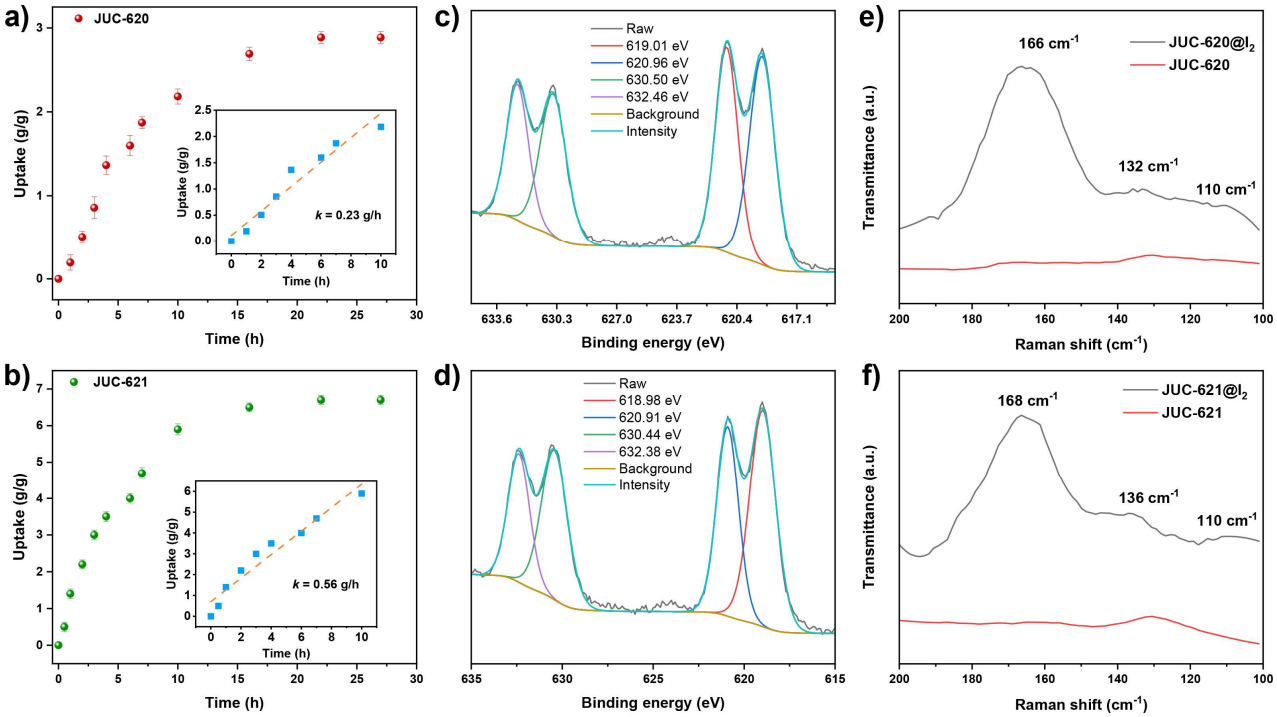

Figure 4. Study of iodine capture. Uptake of I_2 for JUC-620 (a) and JUC-621 (b) as a function of exposure time at 75ºC and ambient pressure. XPS for JUC-620 (c) and JUC-621 (d) after I_2 uptake. Raman spectra of JUC-620 (e) and JUC-621 (f) before (red curve) and after (black curve) I_2 uptake.

were $a = b = 37.260$ Å and $c = 13.350$ Å. In Figure 2a,b, kinematical calculations of SAED along [001] and [100] zone axes of the JUC-621 model matched near perfectly with experimental results. The lattice averaged iDPC-STEM image in *p*1 and *p2mm* symmetry-imposed image also highly agreed with the simulated projective potential (Figure 2d). In order to display the mesoporous channels along [001] direction, a superimposed structure model has been given in Figure 2f. Notably, JUC-621 represents a rare chiral COF framework and the first case of 3D COFs with **qtz** net.

Furthermore, we performed an investigation to explore the transformation between two isomers. To facilitate the transformation, we added excess TFAPPM to promote the process via monomer exchange. In this case, an in-situ transformation was successfully realized from JUC-621 to JUC-620 at different times (12 h, 24 h, 3 days, and 5 days; Figure S23). Conversely, a failed conversion from JUC-620 to JUC-621 was observed (Figure S24). These results demonstrated that JUC-620 might be a thermodynamic product, whereas JUC-621 should be a kinetic product. This hypothesis was also supported by the results of DFT calculations, which indicates that the total energy of JUC-620 is significantly lower than that of JUC-621 (up to 264.3 kcal mol^{-1}).[33,34]

The porosity and specific surface areas of two isomers were proved by nitrogen (N_2) adsorption-desorption isotherms at 77 K. As can be seen in Figure 3a, a rapid N_2 uptake at low relative pressure for JUC-620 was observed ($P/P_0 < 0.01$), which reveals a microporous characteristic. This isotherm was followed by a gradual increase ranging from $P/P_0 = 0.1$ to 0.4, and the significant hysteresis loop was attributable to a guest-induced structural transformation and/or reorientation of the guest packing under increased pressure, which is similar to those typical **dia** nets, such as COF-300 and COF-320.[35,36] In contrast, JUC-621 had a N_2 adsorption at the low pressure of $P/P_0 < 0.05$ along with a second step at $P/P_0 = 0.2$, which is a typical characteristic of mesoporous materials (Figure 3b). According to their N_2 adsorption isotherms, the Brunauer−Emmett−Teller (BET) specific surface area of JUC-621 was as high as 2060 $m^2\ g^{-1}$, which is much higher than that of JUC-620 (980 $m^2\ g^{-1}$, Figures S25 and S26). Furthermore, the pore-size distribution was calculated by nonlocal density functional theory (NLDFT). JUC-621 showed the mesopore with a size of 23 Å, and JUC-620 was only a microporous material with a pore size of 12 Å (Figure 3a,b). The pore-size distribution of both materials was in good agreement with those of crystal structures (13 Å for JUC-620 and 25 Å for JUC-621, respectively). Remarkably, compared to MOFs with the same **qtz** net (Table S2), e.g., 8.6 Å and 150 m^2/g for QMOF-1, 7.8 Å and 190 $m^2\ g^{-1}$ for QMOF-2,[37] 6 Å for $\{(Me_2NH_2)\ [Tb(OBA)_2](Hatz)(H_2O)_{1.5}\}$,[38] and 4.4 Å for In-BDC-NH_2,[39] JUC-621 as a pure organic framework displayed an impressive BET surface area (2060 $m^2\ g^{-1}$) and pore size (up to 23 Å), which indicates that such materials have great potential because of their large channels and high surface areas.

To further demonstrate the different porous specialties of isomers with different topologies, we explored the adsorption of a dye molecule, crystal violet (CV), which is a triangular structure with a molecular size of ~12.0 Å.[40,41] Typically, the samples of JUC-620 and JUC-621 was ultrasonic dispersion (~30 s) in a 20.0 mL aqueous solution of CV (20.0 mg L^{-1}). The amount of CV in the supernatant was monitored through UV-Vis spectrophotometry, and the characteristic absorbance at 583 nm was measured from 0 to 120 mins. As shown in Figure 3c,d, the results displayed a continuous decrease until complete elimination (~100%) of the amount of CV in suspended JUC-621 due to the presence of its mesopores. However, a limited decrease in the amount of CV in suspended JUC-620 (~38%) was observed because of the micropore characteristic of JUC-620 (Figures S27 and S28). JUC-621 can be isolated by centrifugation and reused at least three times almost without loss of adsorption capacity (Figures S29 and S30). The obvious difference in dye adsorption further proved distinct pore characteristics in these COF isomers.

We also conducted the experiment of I_2 adsorption by exposing these isomers to I_2 vapor at 75 ºC under ambient pressure with a humidity of 38%. Both isomers exhibited a nearly linear increment of I_2 adsorption in 10 h, and then reached adsorption saturation within 22 h (Figure 4a,b). Due to the larger pore volume and specific surface area, JUC-621 showed much higher I_2 uptake (6.7 g g^{-1}) and faster I_2 absorption rate (0.56 g h^{-1}) compared to those of JUC-620 (uptake of 2.9 g g^{-1} and absorption rate of 0.23 g h^{-1}), which has surpassed most of porous materials (Table S3), such as 5.20 g g^{-1} for JUC-560, 2.18 g g^{-1} for MOF-808, 4.73 g g^{-1} for HcOFs, and 6.07 g g^{-1} for 60PEI@HCP.[42-45] To investigate the existing state of I_2 in I_2@COFs, we conducted X-ray photoelectron spectroscopy (XPS). Two conspicuous peaks located at 632.46 eV and 620.96 eV for I_2@JUC-620, as well as 632.38 eV and 618.98 eV for I_2@JUC-621, belong to I $3d_{3/2}$ and I $3d_{5/2}$ orbitals of I_2 respectively, and another two peaks at 630.50 eV and 619.01 eV for I_2@JUC-620 as well as 630.44 eV and 620.91 eV for I_2@JUC-621 could be attributed to the formation of polyiodides (such as I_3^- and I_5^-, Figure 4c,d).[42] Furthermore, strong peaks at 166 (or 168), 132 (or 136) and 110 cm^{-1} were observed for I_2@JUC-620 (or I_2@JUC-621) by using the Raman spectra, indicating the stretching vibrations of I_3^- and I_5^- anions (Figure 4e,f). The iodine release process of I_2@COFs in ethanol solution could be detected using a UV spectrophotometer (Figures S31-36), and simultaneously these regenerated COFs maintained good recyclability (Figures S37 and S38).

CONCLUSIONS

In conclusion, for the first time, we designed and synthesized two 3D COFs with topological isomerism, JUC-620 with **dia** net and JUC-621 with **qtz** net, based on a flexible tetrahedral building unit under different solvents. The structures of isomers have been resolved by combining PXRD patterns and high-resolution iDPC-STEM images. To the best of our knowledge, JUC-621 is a rare chiral framework and the first example of 3D COFs with **qtz** topology. Furthermore, these isomers showed an obvious difference in their porous properties. JUC-621 had permanent mesopores (up to ~ 23 Å) and a large surface area (~ 2060 m^2 g^{-1}), which are much higher than those of JUC-620 (pore size of ~12 Å and a surface area of 980 m^2 g^{-1}). In addition, due to the mesoporous channels, JUC-621 could efficiently adsorb dye molecules and exhibited a high I_2 uptake (as high as 6.7 g g^{-1}), which is 2.3 times than that of JUC-620 (~2.9 g g^{-1}). This work not only observes a novel phenomenon of topology isomerism in 3D COFs, but also greatly promotes the study of structure-property relationship of COF materials.

ASSOCIATED CONTENT

Supporting Information

The data that support the findings of this study are available in the supplementary material of this article. http://pubs.acs.org.

Additional experimental details, materials, and methods, including SEM, TEM, FT-IR, solid-state ^{13}C NMR, TGA, PXRD, adsorption results, and unit cell parameters (PDF)

AUTHOR INFORMATION

Corresponding Author

Qianrong Fang − *State Key Laboratory of Inorganic Synthesis and Preparative Chemistry, Jilin University, Changchun 130012, P. R. China; orcid.org/0000-0003-3365-5508; Email: qrfang@jlu.edu.cn*

Daliang Zhang − *Multi-scale Porous Materials Center, Institute of Advanced Interdisciplinary Studies & School of Chemistry and Chemical Engineering, Chongqing University, Chongqing 400044, P. R. China; orcid.org/0000-0003-3494-7000; Email: daliang.zhang@cqu.edu.cn*

Yujie Wang − *State Key Laboratory of Inorganic Synthesis and Preparative Chemistry, Jilin University, Changchun 130012, P. R. China; orcid.org/0000-0003-2736-1087; Email: wyujie@jlu.edu.cn*

Author

Yaozu Liu − *State Key Laboratory of Inorganic Synthesis and Preparative Chemistry, Jilin University, Changchun 130012, P. R. China*

Jingwei Li − *Multi-scale Porous Materials Center, Institute of Advanced Interdisciplinary Studies & School of Chemistry and Chemical Engineering, Chongqing University, Chongqing 400044, P. R. China*

Jia Lv − *Multi-scale Porous Materials Center, Institute of Advanced Interdisciplinary Studies & School of Chemistry and Chemical Engineering, Chongqing University, Chongqing 400044, P. R. China*

Zitao Wang − *State Key Laboratory of Inorganic Synthesis and Preparative Chemistry, Jilin University, Changchun 130012, P. R. China*

Jinquan Suo − *State Key Laboratory of Inorganic Synthesis and Preparative Chemistry, Jilin University, Changchun 130012, P. R. China*

Junxia Ren − *State Key Laboratory of Inorganic Synthesis and Preparative Chemistry, Jilin University, Changchun 130012, P. R. China*

Jianchuan Liu − *State Key Laboratory of Inorganic Synthesis and Preparative Chemistry, Jilin University, Changchun 130012, P. R. China*

Dong Liu − *Multi-scale Porous Materials Center, Institute of Advanced Interdisciplinary Studies & School of Chemistry and Chemical Engineering, Chongqing University, Chongqing 400044, P. R. China*

Valentin Valtchev − *Qingdao Institute of Bioenergy and Bioprocess Technology, Chinese Academy of Sciences Qingdao, Shandong 266101, P. R. China; Normandie Univ, ENSICAEN, UNICAEN, CNRS, Laboratoire Catalyse et Spectrochimie, Caen 14050, France*

Shilun Qiu − *State Key Laboratory of Inorganic Synthesis and Preparative Chemistry, Jilin University, Changchun 130012, P. R. China*

Author Contributions

§Y.L. and J.L. contributed equally to this work.

Notes

The authors declare no competing financial interests.

ACKNOWLEDGMENTS

This work was supported by National Key R&D Program of China (2022YFB3704900 and 2021YFF0500500), National Natural Science Foundation of China (22025504, 21621001, and 22105082), the SINOPEC Research Institute of Petroleum Processing, "111" project (BP0719036 and B17020), China Postdoctoral Science Foundation (2020TQ0118 and 2020M681034), and the program for JLU Science and Technology Innovative Research Team. V.V., Q.F. and S.Q. acknowledge the collaboration in the Sino-French International Research Network “Zeolites”.

REFERENCES

(1) Calvey, T. N., Isomerism and anaesthetic drugs. *Acta. Anaesth. Scand.* **1995,** *106*, 83-90.

(2) Chhabra, N.; Aseri, M. L.; Padmanabhan, D., A review of drug isomerism and its significance. *Int. J. Appl. Basic. Med.* **2013,** *3*, 16-8.

(3) Makal, T. A.; Yakovenko, A. A.; Zhou, H.-C., Isomerism in Metal-Organic Frameworks: "Framework Isomers". *J. Phys. Chem. Lett.* **2011,** *2*, 1682-1689.
(4) Cote, A. P.; Benin, A. I.; Ockwig, N. W.; O'Keeffe, M.; Matzger, A. J.; Yaghi, O. M., Porous, crystalline, covalent organic frameworks. *Science* **2005,** *310*, 1166-1170.
(5) Colson, J. W.; Woll, A. R.; Mukherjee, A.; Levendorf, M. P.; Spitler, E. L.; Shields, V. B.; Spencer, M. G.; Park, J.; Dichtel, W. R. Oriented 2D Covalent Organic Framework Thin Films on Single-Layer Graphene. *Science* **2011**, *332*, 228-231.
(6) Guan, X.; Chen, F.; Fang, Q.; Qiu, S., Design and applications of three dimensional covalent organic frameworks. *Chem. Soc. Rev.* **2020,** *49*, 1357-1384.
(7) Tao, S.; Jiang, D., Covalent Organic Frameworks for Energy Conversions: Current Status, Challenges, and Perspectives. *CCS Chem* **2021,** *3*, 2003-2024.
(8) Gan, J.; Bagheri, A. R.; Aramesh, N.; Gul, I.; Franco, M.; Almulaiky, Y. Q.; Bilal, M., Covalent organic frameworks as emerging host platforms for enzyme immobilization and robust biocatalysis - A review. *Int. J. Biol. Macromol.* **2021,** *167*, 502-515.
(9) Han, X.; Yuan, C.; Hou, B.; Liu, L.; Li, H.; Liu, Y.; Cui, Y., Chiral covalent organic frameworks: design, synthesis and property. *Chem. Soc. Rev.* **2020,** *49*, 6248-6272.
(10) Wang, Y.; Liu, Y.; Li, H.; Guan, X.; Xue, M.; Yan, Y.; Valtchev, V.; Qiu, S.; Fang, Q., Three-Dimensional Mesoporous Covalent Organic Frameworks through Steric Hindrance Engineering. *J. Am. Chem. Soc.* **2020,** *142*, 3736-3741.
(11) Wang, Z.; Zhang, S.; Chen, Y.; Zhang, Z.; Ma, S., Covalent organic frameworks for separation applications. *Chem. Soc. Rev.* **2020,** *49*, 708-735.
(12) Yang, Q.; Luo, M.; Liu, K.; Cao, H.; Yan, H., Covalent organic frameworks for photocatalytic applications. *Appl. Catal. B* **2020,** *276*.
(13) Zhao, X.; Pachfule, P.; Thomas, A., Covalent organic frameworks (COFs) for electrochemical applications. *Chem. Soc. Rev.* **2021,** *50*, 6871-6913.
(14) Chen, R.; Shi, J.; Ma, Y.; Lin, G.; Lang, X.; Wang, C., Designed Synthesis of a 2D Porphyrin-Based sp^2 Carbon-Conjugated Covalent Organic Framework for Heterogeneous Photocatalysis. *Angew. Chem. Int. Ed.* **2019,** *61*, 6430-6434.
(15) Zhang, L.; Yi, L.; Sun, Z-J.; Deng, H., Covalent Organic Frameworks for Optical Applications. *Aggregate* **2020**, 2006844.
(16) Wang, D.-G.; Qiu, T.; Guo, W.; Liang, Z.; Tabassum, H.; Xia, D.; Zou, R., Covalent organic framework-based materials for energy applications. *Energ Environ. Sci.* **2021,** *14*, 688-728.
(17) Wang, G.-B.; Li, S.; Yan, C.-X.; Zhu, F.-C.; Lin, Q.-Q.; Xie, K.-H.; Geng, Y.; Dong, Y.-B., Covalent organic frameworks: emerging high-performance platforms for efficient photocatalytic applications. *J Mater. Chem. A* **2020,** *8*, 6957-6983.
(18) Liu, Y.; Ren, J.; Wang, Y.; Zhu, X.; Guan, X.; Wang, Z.; Zhou, Y.; Zhu, L.; Qiu, S.; Xiao, S.; Fang, Q., A Stable Luminescent Covalent Organic Framework Nanosheet for Sensitive Molecular Recognition. *CCS Chem.* **2023,** doi.org/10.31635/ccschem.022.202202352.
(19) Chandra, S.; Kundu, T.; Kandambeth, S.; BabaRao, R.; Marathe, M. Y.; Kunjir, S. M.; Banerjee, R. Phosphoric Acid Loaded Azo (−N=N−) Based Covalent Organic Framework for Proton Conduction. *J. Am. Chem. Soc.* **2014**, *136*, 6570-6573.
(20) Xian, W.; Zhang, P.; Zhu, C.; Zuo, X.; Ma, S.; Sun, Q., Bionic Thermosensation Inspired Temperature Gradient Sensor Based on Covalent Organic Framework Nanofluidic Membrane with Ultrahigh Sensitivity. *CCS Chem* **2021,** *3*, 2464-2472.
(21) Tang, X.; Chen, Z.; Xu, Q.; Su, Y.; Xu, H.; Horike, S.; Zhang, H.; Li, Y.; Gu, C., Design of Photothermal Covalent Organic Frameworks by Radical Immobilization. *CCS Chem* **2022,** *4*, 2842-2853.
(22) Meng, Y.; Luo, Y.; Shi, J.-L.; Ding, H.; Lang, X.; Chen, W.; Zheng, A.; Sun, J.; Wang, C., 2D and 3D Porphyrinic Covalent Organic Frameworks: The Influence of Dimensionality on Functionality. *Angew. Chem. Int. Ed.* **2020,** *59*, 3624-3629.
(23) Ma, T.; Li, J.; Niu, J.; Zhang, L.; Etman, A. S.; Lin, C.; Shi, D.; Chen, P.; Li, L.-H.; Du, X.; Sun, J.; Wang, W., Observation of Interpenetration Isomerism in Covalent Organic Frameworks. *J. Am. Chem. Soc.* **2018,** *140*, 6763-6766.
(24) Li, H.; Ding, J.; Guan, X.; Chen, F.; Li, C.; Zhu, L.; Xue, M.; Yuan, D.; Valtchev, V.; Yan, Y.; Qiu, S.; Fang, Q., Three-Dimensional Large-Pore Covalent Organic Framework with stp Topology. *J. Am. Chem. Soc.* **2020,** *142*, 13334-13338.
(25) Li, H.; Chen, F.; Guan, X.; Li, J.; Li, C.; Tang, B.; Valtchev, V.; Yan, Y.; Qiu, S.; Fang, Q., Three-Dimensional Triptycene-Based Covalent Organic Frameworks with ceq or acs Topology. *J. Am. Chem. Soc.* **2021,** *143*, 2654-2659.
(26) Yu, C.; Li, H.; Wang, Y.; Suo, J.; Guan, X.; Wang, R.; Valtchev, V.; Yan, Y.; Qiu, S.; Fang, Q., Three-Dimensional Triptycene-Functionalized Covalent Organic Frameworks with hea Net for Hydrogen Adsorption. *Angew. Chem. Int. Ed.* **2022,** *61,* e202117101.
(27) Liu, Y.; Chen, P.; Wang, Y.; Suo, J.; Ding, J.; Zhu, L.; Valtchev, V.; Yan, Y.; Qiu, S.; Sun, J.; Fang, Q., Design and Synthesis of a Zeolitic Organic Framework. *Angew. Chem. Int. Ed.* **2022**. *61*. e2022035.
(28) Yaghi, O. Reticular Chemistry–Construction, Properties, and Precision Reactions of Frameworks. *J. Am. Chem. Soc.* **2016,** *138*, 15507-15509.
(29) Yaghi, O. Reticular Chemistry in All Dimensions. *ACS Cent. Sci.* **2019**, *5*, 1295-1300.
(30) Huang, X.-C.; Zhang, J.-P.; Lin, Y.-Y.; Chen, X.-M., Triple-stranded helices and zigzag chains of copper(i) 2-ethylimidazolate: solvent polarity-induced supramolecular isomerism. *Chem. Commun.* **2005**, 2232-2234.
(31) Hovmöller S. CRISP: Crystallographic Image Processing on a Personal Computer, *Ultramicroscopy* **1992**, *41*, 121-135.
(32) Momma K.; Izumi, F. VESTA 3 for Three-Dimensional Visualization of Crystal, Volumetric and Morphology Data. *J. Appl. Crystallogr.* **2011**, *44*, 1272-1276.
(33) Borstnik, U.; VandeVondele, J.; Weber, V.; Hutter, J., Sparse matrix multiplication: The distributed block-compressed sparse row library. *Parallel Comput.* **2014**, *40*, 47-58.
(34) Gaussian 09 Rev. B.01 *Wallingford, CT* **2009**.
(35) Uribe-Romo, F. J.; Hunt, J. R.; Furukawa, H.; Klock, C.; O'Keeffe, M.; Yaghi, O. M., A Crystalline Imine-Linked 3-D Porous Covalent Organic Framework. *J. Am. Chem. Soc.* **2009,** *131*, 4570-4571.
(36) Zhang, Y-B.; Su, J.; Furukawa, H.; Yun, Y.; Gándara, F.; Duong, A.; Zou, X.; Yaghi, O. M., Single-Crystal Structure of a Covalent Organic Framework. *J. Am. Chem. Soc.* **2013,** *135*, 16336-16339.
(37) Sun, J. Y.; Weng, L. H.; Zhou, Y. M.; Chen, J. X.; Chen, Z. X.; Liu, Z. C.; Zhao, D. Y., QMOF-1 and QMOF-2: Three-dimensional metal-organic open frameworks with a quartzlike topology. *Angew. Chem. Int. Ed.* **2002,** *41*, 4471-4473.
(38) Chen, D.-M.; Zhang, N.-N.; Liu, C.-S.; Du, M., Template-directed synthesis of a luminescent Tb-MOF material for highly selective Fe^{3+} and Al^{3+} ion detection and VOC vapor sensing. *J. Mater. Chem. C* **2017,** *5*, 2311-2317.
(39) Krueger, M.; Albat, M.; Inge, A. K.; Stock, N., Investigation of the effect of polar functional groups on the crystal structures of indium MOFs. *Crystengcomm* **2017,** *19*, 4622-4628.
(40) Song, J.; Wang, Z.; Liu, Y.; Tuo, C.; Wang, Y.; Fang, Q.; Qiu, S., A Three-dimensional Covalent Organic Framework for CO_2 Uptake and Dyes Adsorption. *Chem. Research Chinese U.* **2022,** *38*, 834-837.
(41) Wang, Z.; Liu, Y.; Wang, Y.; Fang, Q., A New Covalent Organic Framework Modified with Sulfonic Acid for CO_2 Uptake and Selective Dye Adsorption. *Acta Chim Sinica* **2022,** *80*, 37-43.

(42) Chang, J. H.; Li, H.; Zhao, J.; Guan, X. Y.; Li, C. M.; Yu, G. T.; Valtchev, V.; Yan, Y. S.; Qiu, S. L.; Fang, Q. R., Tetrathiafulvalene-based covalent organic frameworks for ultrahigh iodine capture. *Chem. Sci.* **2021,** *12*, 8452-8457.
(43) Chen, P.; He, X.; Pang, M.; Dong, X.; Zhao, S.; Zhang, W., Iodine Capture Using Zr-Based Metal-Organic Frameworks (Zr-MOFs): Adsorption Performance and Mechanism. *Acs Appl. Mater. Interfaces* **2020,** *12*, 20429-20439.
(44) Jiang, X.; Cui, X.; Duncan, A. J. E.; Li, L.; Hughes, R. P.; Staples, R. J.; Alexandrov, E. V.; Proserpio, D. M.; Wu, Y.; Ke, C., Topochemical Synthesis of Single-Crystalline Hydrogen-Bonded Cross-Linked Organic Frameworks and Their Guest-Induced Elastic Expansion. *J. Am. Chem. Soc.* **2019,** *141*, 10915-10923.
(45) Li, X.; Chen, G.; Jia, Q., Highly efficient iodine capture by task-specific polyethylenimine impregnated hypercrosslinked polymers. *J. Taiwan Inst. Chem E* **2018,** *93*, 660-666.

TOC Graphic:

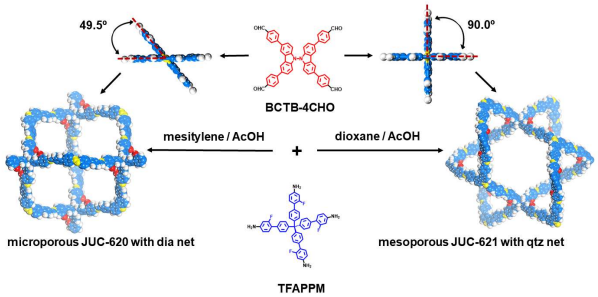
49.5°
90.0°
BCTB-4CHO
mesitylene / AcOH
dioxane / AcOH
+
microporous JUC-620 with dia net
mesoporous JUC-621 with qtz net
TFAPPM